https://doi.org/10.5194/egusphere-2025-1307
Preprint. Discussion started: 27 March 2025

Abrupt meteorological changes reverse thermohaline features in the skin layer

Lisa Gassen[1], Samuel M. Ayim[1], Leonie Jaeger[1], Jens Meyerjürgens[1], Mariana Ribas-Ribas[1], Oliver Wurl[1]

[1]Center of Marine Sensors, Institute for Chemistry and Biology of the Marine Environment, Carl von Ossietzky University of Oldenburg, Wilhelmshaven, Germany

Correspondence to: Lisa Gassen (lisa.gassen-bertzbach@uol.de)

Abstract. This study provides unique data on temperature and salinity anomalies between the skin layer (upper first millimetre) and a depth of 100 cm during abrupt meteorological changes—that is, shifts in air temperature, wind speed, precipitation, and heat fluxes. We determined how these abrupt meteorological changes forced the anomalies and altered the conditions at the air–sea boundary layer during three events monitored by an autonomous surface vehicle. Two events were observed in the harbour of Bremerhaven and one event in the North Sea. The skin layer, which covers the upper millimetre of the sea surface, interacts with the atmosphere, including heat, gas, and freshwater fluxes. The characteristics of the skin layer regulate the exchange of heat and gases between the atmosphere and the ocean. Global climate change increases extreme weather events, highlighting the need for observations during abrupt shifts to better estimate heat flux changes. However, there is a lack of small-scale mechanistic understanding of these fluxes, especially under abrupt meteorological changes, due to observational challenges during stormy conditions in the open sea. Here, we show that the skin layer instantly reacts to abrupt meteorological changes. The average temperature change in the skin layer was almost 50% higher than that at a depth of 100 cm. An abrupt change in meteorological conditions, shifting the net heat flux from positive to negative, can turn a warm skin layer into a cooler layer compared with the 100 cm depth. The effect of abrupt meteorological changes, including freshwater fluxes, on salinity anomalies was less pronounced in the harbour than in the North Sea event. The current velocities showed that changes in wind direction could alter the surface current direction, and that the backscatter signal consistently reflects wind-induced mixing, with higher backscatter observed during increased wind conditions. This study reveals the complex relationships between atmospheric conditions and oceanic responses and provides valuable information for understanding air–sea interactions and their implications for climate dynamics.

https://doi.org/10.5194/egusphere-2025-1307
Preprint. Discussion started: 27 March 2025

1 Introduction

The skin layer of the ocean represents the boundary between the atmosphere and the ocean and typically has a thickness of approximately 1 mm (Liss et al., 1997; Wurl et al., 2009). The characteristics of the skin layer are responsible for regulating the exchange of gases, heat, and freshwater between the atmosphere and the ocean (Fairall et al., 1996b; Liss and Duce, 1997; Gassen et al., 2023). Skin temperature is a critical indicator of gas and heat flux exchange processes (Fairall et al., 1996b). The skin layer is usually cooler than the underlying near-surface layer (NSL) (first upper 100 cm) because of heat loss from the ocean to the atmosphere (Katsaros and Buettner, 1969; Schluessel et al., 1990; Zappa et al., 1998). This cool skin layer remains in the presence of a diurnal thermocline (Minnett, 2003; Jessup et al., 1997; Yu, 2007). The cooling effect significantly affects gas solubility in the skin layer (Watson et al., 2020). A warmer skin develops in the case of a positive net heat flux within the skin layer (Katsaros, 1980). Skin salinity is a key parameter for monitoring freshwater fluxes (evaporation–precipitation) over the ocean; adding or removing freshwater to or from the surface through precipitation and evaporation results in changes in surface salinity (Durack, 2015; Gassen et al., 2023; Gassen et al., 2024b). In the same processes, freshwater fluxes affect skin temperature. Evaporation releases heat from the sea surface into the atmosphere. Conversely, precipitation typically has a different temperature from the ocean surface, potentially altering the surface temperature (Gosnell et al., 1995; Williams and Stanfill, 2002). Moreover, precipitation reduces the gas transfer velocity on the surface (Ho et al., 2004).

Considerable research has been conducted on thermal stratification induced by diurnal warming, heat exchange processes, and wind-driven turbulent mixing in the NSL (Price et al., 1986; Fairall et al., 1996b; Gentemann et al., 2003). However, there have been comparatively few investigations into the effects of these processes on the skin layer. To achieve reliable outputs for atmospheric models of ocean heat fluxes, an accuracy of approximately 10 W m^{-2} is required (Fairall et al., 1996a). However, the scarcity of *in situ* measurements is a significant challenge, particularly given the difficulties in observing them, such as using accurate instruments during extreme meteorological events. Observing such events in the open sea is challenging as research vessels typically avoid deploying oceanographic equipment during unfavourable weather conditions. For example, measurements of the skin layer temperature and salinity during rapid meteorological shifts (e.g., in wind speed and air temperature) are lacking at high temporal and spatial resolutions. This limits our understanding of the immediate response mechanisms in the skin layer. At the same time, global climate change is responsible for an increase in the frequency of extreme meteorological events (Allen and Ingram, 2002; Ummenhofer and Meehl, 2017), making observations during abrupt meteorological shifts increasingly critical to better estimate the resulting changes in heat fluxes.

However, the potential consequences of heat, gas and freshwater fluxes during rapid meteorological changes remain uncertain. Rapid meteorological changes often occur concurrently with increasing wind speeds (Webster et al., 1996; Ten Doeschate et al., 2019). The influence of wind speed on thermohaline stratification and mixing processes on the sea surface has been the subject of several studies (Leibovich, 1983; Soloviev et al., 2014). However, very little is known about small-scale dynamics in the skin layer and the occurrence of fast mixing processes. Previous studies have indicated that the skin layer is affected by freshwater fluxes (Wurl et al., 2019; Gassen et al., 2023; Gassen et al., 2024a), and stratification in the upper first metre of the

https://doi.org/10.5194/egusphere-2025-1307
Preprint. Discussion started: 27 March 2025

surface is disrupted at wind speeds of more than 5 m s^{-1} (Moulin et al., 2021; Gassen et al., 2024b). Despite these previous studies, the specific effects of abrupt meteorological changes, such as rapid wind speed and air temperature shifts, on temperature and salinity anomalies between the skin layer and 100 cm (skin −100 cm) remain poorly characterized. There is a need for detailed observational data on how rapid meteorological changes affect skin layer dynamics to improve the accuracy of climate models, especially in predicting the immediate responses of the skin layer to extreme meteorological events (Renfrew et al., 2002).

This study aims to investigate the effects of rapid meteorological changes on temperature and salinity anomalies, addressing a gap in the current understanding of skin layer dynamics under extreme meteorological conditions. Our measurements include recording relevant meteorological variables, such as wind speed and air temperature, and calculating heat and freshwater fluxes. Furthermore, our study measured near-surface currents and observed temperature and salinity in the skin layer and the NSL. These measurements were conducted during rapid meteorological changes in the harbour of Bremerhaven, Germany, and in the North Sea. Even though *in situ* observation data during rapid meteorological changes were extremely rare, we were able to record three events. The responses of temperature and salinity anomalies to rapid meteorological changes were determined. The consequences of heat and freshwater fluxes in the skin layer and mixing processes were also analysed. This approach aims to contribute to a more nuanced understanding of skin layer dynamics and to enhance the accuracy of atmospheric models by providing empirical data on the skin layer's responses to sudden meteorological changes. Our findings can improve and refine future observational strategies for air–sea interactions and models.

2 Materials and Methods

During the course of cruise HE614 of RV *Heincke*, temperature and salinity changes were recorded using the autonomous surface vehicle (ASV) *HALOBATES* (Wurl et al., 2024) during the three events of rapid meteorological changes. Two events occurred in the harbour of Bremerhaven (53.52°N, 8.58°E) on 14 and 15 March 2023, respectively. The ASV can be operated manually with remote control or autonomously through a pre-programmed mission. Due to space constraints in the harbour, the ASV was operated manually using a remote control within a few hundred metres of the berth of the research vessel (Fig. S1). An abrupt meteorological change event during a previous RV *Heincke* cruise (HE609) in the North Sea (53.85°N, 7.68°E) was also analysed. On 10 October 2022, the ASV was operated when a rapid meteorological change occurred. The ASV drifted during operational time (Gassen et al., 2024b). Here, we referred to abrupt meteorological changes as changes in wind speed of > 0.3 m s^{-1} min^{-1}.

The ASV was equipped with six rotating glass discs. The skin of the water surface adhered to the glass discs (Shinki et al., 2012; Ribas-Ribas et al., 2017) and was sampled in a flow-through system to continuously measure temperature and conductivity (Ocean Seven310, Idronaut, Italy), which were later used for absolute salinity calculations. According to the manufacturer datasheet, the sensors have an accuracy of 0.0015 mS cm^{-1} and 0.0015 °C for temperature and conductivity, respectively. Water from a 100 cm depth was sampled and pumped through the temperature and conductivity probes (Wurl et

https://doi.org/10.5194/egusphere-2025-1307
Preprint. Discussion started: 27 March 2025

al., 2024). Temperature and salinity anomalies (ΔT, ΔS) were calculated as the difference between the values from the skin layer (T_{skin}, S_{skin}) and those from the 100 cm depth ($T_{100\,cm}$, $S_{100\,cm}$):

$$\Delta T = T_{skin} - T_{100\,cm} \quad (1)$$

$$\Delta S = S_{skin} - S_{100\,cm} \quad (2)$$

Density was calculated using the Thermodynamic Equation of Seawater 2010 (TEOS-10) and the Gibbs-SeaWater Oceanographic package for R (Mcdougall and Barker, 2011). *HALOBATES* has two weather stations at a height of 2 m to determine meteorological variables, such as air temperature, humidity, and wind speed. One of the weather stations (Campbell Scientific Ltd., Model CR1000X, United Kingdom) measures at 10 s intervals, and the other (Thies Clima, Model SMP6, Germany) measures at 10 min intervals. For the station in the North Sea, we used data from the Thies Clima weather station because of a technical failure of the weather station from Campbell Scientific.

Two pyrgeometers and pyranometers (IR20 and SR20; Hukseflux, Netherlands) were installed on the RV *Heincke* to measure the downward and upward longwave irradiances. To compute the heat fluxes and evaporation rates, the COARE 3.6 algorithm was applied (Fairall et al., 2003). Net heat flux was calculated as the sum of the longwave, shortwave, latent and sensible heat fluxes. Given that the measuring interval of the radiometers was set to 10 min, linear interpolation was applied to obtain values at 10 s intervals for the harbour events. An optical laser disdrometer (Thies Clima, 5.4110.xx.x00, Germany) was installed on the upper deck of the research vessel to monitor precipitation intensity and accumulated precipitation.

Acoustic Doppler current profiler (ADCP) data were recorded at a frequency of 2 Hz, providing accurate estimates of current velocities that were referenced to the GPS position data. A 600-kHz Teledyne RD Instruments RiverRay ADCP was mounted at the centre and beneath the ASV and was configured with a 0.2 m bin size and a blanking distance of one cell (0.2 m) beyond the immersion depth of 0.3 m. This configuration provided the first data bin at a depth of 0.5 m.

A Pearson correlation analysis was conducted with the derived temperature and salinity anomalies and essential variables, such as air temperature, wind speed, precipitation intensity, net heat flux, and backscatter velocity. The results were considered significant when $p < 0.05$, with a 95% confidence level. The correlation was considered strong, with correlation coefficients ranging from 0.7 to 1 or from –0.7 to –1. The duration and intensity of the meteorological changes differed between the harbour and North Sea events. For this reason, a correlation analysis of all the main variables with possible relationships with temperature and salinity anomalies was conducted separately for each event.

https://doi.org/10.5194/egusphere-2025-1307
Preprint. Discussion started: 27 March 2025

3 Results

Table 1 summarizes the total changes in temperature and salinity in the skin layer and at the 100 cm depth and in the meteorological variables during all abrupt meteorological changes. On 15 March 2023, three abrupt changes in wind speeds were observed. These changes are described in Sections 3.1, 3.2, and 3.3.

Table 1 *Total change in temperature and salinity of the skin layer and the 100 cm depth, and the change in meteorological variables during all abrupt weather shifts.*

Event	Change in skin temperature (°C)	Change in 100 cm temperature (°C)	Change in Skin salinity (g kg^{-1})	Change in 100 cm salinity (g kg^{-1})	Change in air temperature (°C)	Change in wind speed (m s^{-1})	Change in precipitation intensity (mm h^{-1})	Change in net heat flux (W m^{-2})
14 March 2023	–0.57	–0.37	+0.10	+0.12	–4.3	+8.55	+7.26	–121
15 March 2023 - A	–0.32	–0.74	–0.16	–0.43	–0.5	+6.53	+0.09	–81
15 March 2023 - B	–0.29	–0.08	–0.15	–0.09	–1.4	+10.69	+0.37	–182
15 March 2023 - C	–0.40	–0.23	+0.10	+0.06	–2.4	+9.21	+1.24	–252
10 October 2022	–0.16	–0.07	–0.17	–0.03	–1.7	+9.20	+10.37	–100

3.1 Harbour event on 14 March 2023

3.1.1 Thermohaline features during abrupt meteorological changes

Meteorological conditions changed abruptly during the first event on 14 March 2023 in the harbour of Bremerhaven between 08:18 and 08:31 UTC (Fig. 1e–g). This was caused by rapid shifts in meteorological variables, such as wind speed and air temperature (Fig. 1e). Before the arrival of the weather front at the location of the ASV, the average air temperature remained constant at 9.24 ± 0.06 °C. With the approach of the weather front, there was a notable decrease in air temperature between 08:19 and 08:25 UTC (i.e., within 8 min), reaching a minimum of 4.30 °C. Afterwards, the air temperature decreased further, but slower, from 4.9 °C to 2.9 °C within 40 min (Fig. 1e). Before the abrupt weather change, light precipitation and wind speed were observed, with mean intensities of 0.26 ± 0.24 mm h^{-1} and 4.41 ± 1.19 m s^{-1}, respectively (Fig. 1e, g). During the abrupt meteorological change, the precipitation rate and wind speed increased notably by 7.26 mm h^{-1} and 8.55 m s^{-1}, respectively.

https://doi.org/10.5194/egusphere-2025-1307
Preprint. Discussion started: 27 March 2025

Simultaneously, there was a change in wind direction from South–South–West to North–North–West (Fig. S2). Following the abrupt meteorological change, the mean wind speed remained high at 7.40 ± 1.94 m s^{-1}, with a maximum wind speed of 12.24 m s^{-1} at 08:39 UTC. In general, the precipitation rate was relatively low, with a mean intensity of 0.39 ± 0.36 mm h^{-1} after the abrupt meteorological change (Fig. 1g). At 08:21 UTC, the evaporation rate shifted from negative to positive values—that is, from condensation to evaporation. Prior to the abrupt meteorological change, the mean evaporation rate was –0.01 ± 0.01 mm h^{-1}, and it increased to 0.05 ± 0.01 mm h^{-1} after the meteorological change (Fig. 1g). Figure S3 shows that the accumulated precipitation exceeded the accumulated evaporation during the operational time of the ASV.

During the abrupt meteorological shift on 14 March 2023, the sea surface temperature decreased, whereas the salinity and density increased following an abrupt change in weather conditions (Fig. 1a–c). Before the abrupt meteorological shift (Fig. 1e–g), the skin layer was cooler than at the 100 cm depth, with a mean temperature anomaly of –0.09 ± 0.03 °C (Fig. 1d). From 08:19 to 08:24 UTC, a rapid decrease in temperature was observed across the skin layer and 100 cm depth, with the most notable decrease occurring in the skin layer (–0.50 °C). Following the abrupt meteorological change, cooler skin developed, exhibiting a maximum skin temperature anomaly of –0.44 °C. After the abrupt meteorological change at 8:18 UTC, the mean skin temperature anomaly during the subsequent period (08:28–09:29 UTC) was –0.35 ± 0.04 °C. At 09:15 UTC, the skin temperature increased, which caused an increase of approximately 0.1 °C in the temperature anomaly.

Before the abrupt meteorological shift, the salinity exhibited minimal variation across the skin layer and the 100 cm depth at a mean skin salinity of 9.34 ± 0.04 g kg^{-1}. After the abrupt change in meteorological conditions (Fig. 1e–g), a notable increase in salinity was observed at all depths at 08:25 UTC. At 08:28 UTC, there was a decrease in salinity for 2 min, followed by a subsequent increase. Following the abrupt meteorological change, the mean absolute skin salinity reached a value of 9.47 ± 0.44 g kg^{-1}. Throughout this occurrence, the salinity of the skin was consistently higher than that at the 100 cm depth. Consequently, the salinity anomaly remained positive—that is, the salinity of the skin remained continuously saltier than that at the 100 cm depth (Fig. 1d). The density graphs mirrored the pattern observed in absolute salinity, indicating an increase in density in the skin layer and at the 100 cm depth following an abrupt meteorological change (Fig. 1c). The mean density was 1007.41 ± 0.25 kg m^{-3} in the skin layer and 1007.36 ± 0.25 kg m^{-3} at the 100 cm depth for the entire operation time, respectively.

Before the abrupt meteorological change, all surface heat fluxes were positive, thus warming the ocean (Fig. 1f), with a mean latent heat flux of 10 ± 4 W m^{-2}, sensible heat flux of 22 ± 8 W m^{-2}, longwave heat flux of 3 ± 1 W m^{-2} and overall net heat flux of 79 ± 14 W m^{-2}. With the onset of the cold weather front, the heat fluxes turned, resulting in a mean latent heat flux of –33 ± 9 W m^{-2}, sensible heat flux of –20 ± 9 W m^{-2}, longwave heat flux of –11 ± 1 W m^{-2} and net heat flux of –3 ± 17 W m^{-2}. The net solar radiation decreased shortly during the abrupt meteorological shift from 49 to 39 W m^{-2} but continued to increase afterwards. The mean shortwave heat flux was 44 ± 5 W m^{-2} before the abrupt change in meteorological variables and 58 ± 6 W m^{-2} after the change.

https://doi.org/10.5194/egusphere-2025-1307
Preprint. Discussion started: 27 March 2025

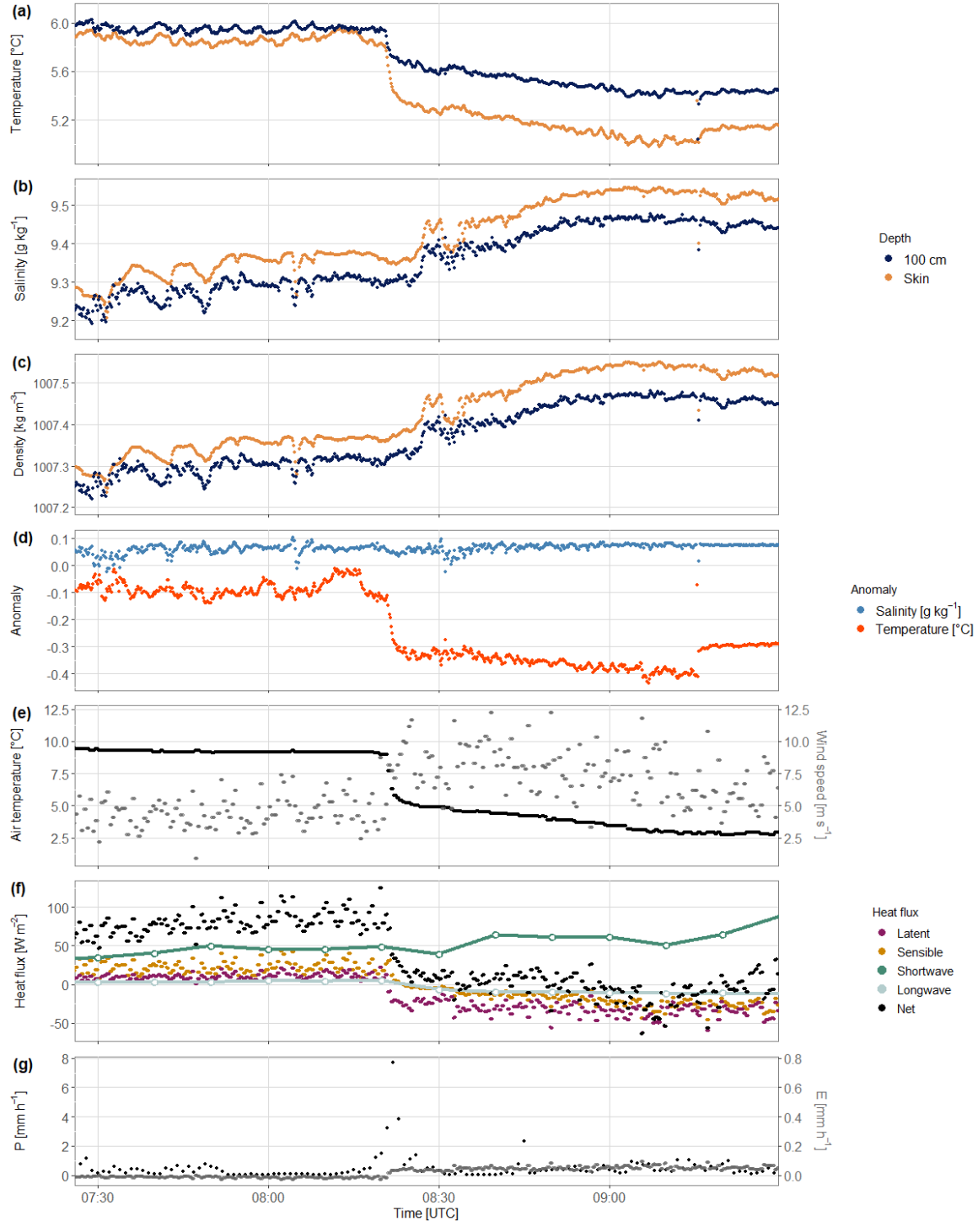

Figure 1: Time series of (a) sea surface temperature, (b) sea surface salinity, (c) sea surface density, (d) temperature and salinity anomaly, (e) air temperature and wind speed, (f) heat flux components, (g) precipitation (P) and evaporation (E) rates on 14 March 2023.

https://doi.org/10.5194/egusphere-2025-1307
Preprint. Discussion started: 27 March 2025

3.1.2 Current velocities on the surface

Figure 2 presents the time-depth plots derived from the ADCP data collected on 14 March 2023, showing the zonal and meridional velocity components and backscatter intensity from 07:30 to 09:30 UTC. The zonal velocity component (Fig. 2a) shows a westward flow from 07:30 to 08:25 UTC, followed by an abrupt shift to an eastward flow with a pronounced current shear at an approximately 3 m depth. The meridional velocity component (Fig. 2b) indicates a northward flow from the surface to a depth of 2 m and a southward flow below 3 m during the same period. After 08:25 UTC, the flow shifted, with the surface current turning southward and the current below 3 m turning northward.

The backscatter intensity (Fig. 2c) shows variations in signal strength across depth and time. It shows a noticeable shift at 08:20 UTC, with an increase in intensity near the surface. This signal aligns with the precipitation event, indicating the wet deposition of atmospheric particles on the surface. Below the surface, the backscatter remains relatively stable with less pronounced changes over time.

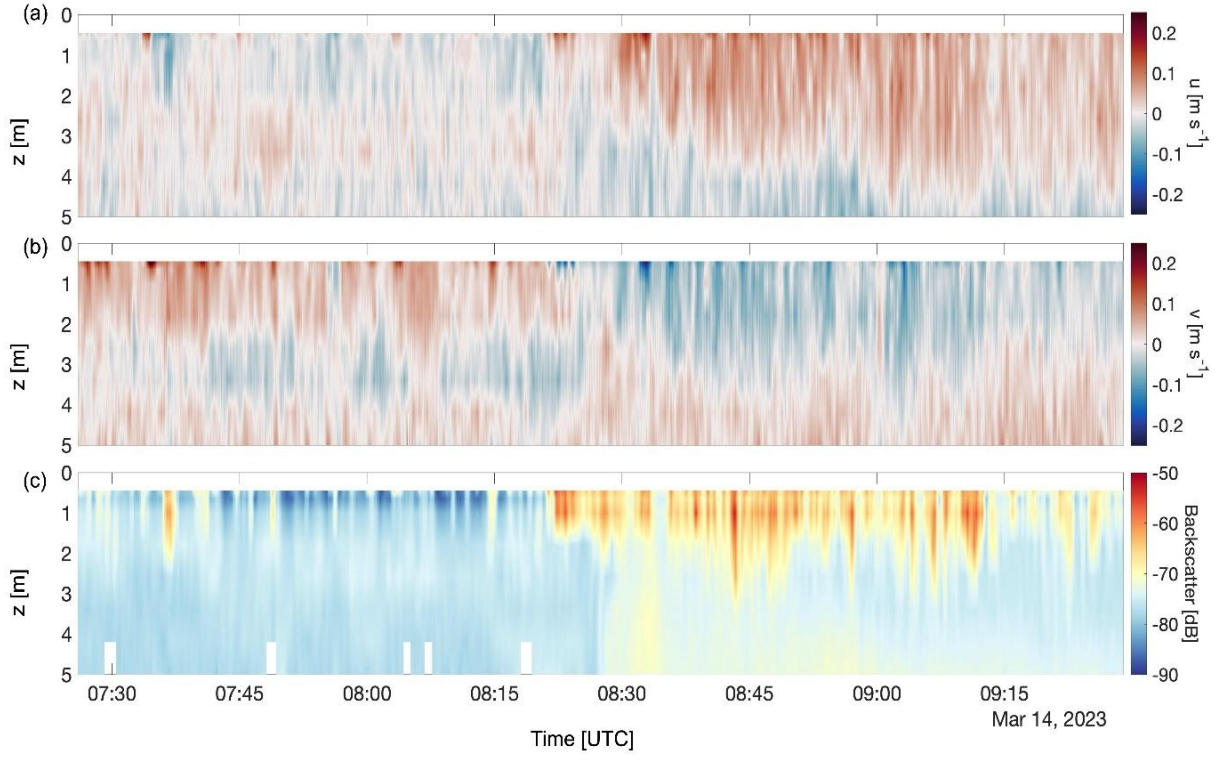

Figure 2: Current velocity data measured with an ADCP mounted at the centre of HALOBATES on 14 March 2023. (a) Zonal current velocity, (b) meridional current velocity and (c) backscatter signals are shown in three panels, and the colour scale shows the velocity magnitude for each current velocity component.

https://doi.org/10.5194/egusphere-2025-1307
Preprint. Discussion started: 27 March 2025

3.2. Harbour event on 15 March 2023

3.2.1 Thermohaline features during abrupt meteorological changes

On 15 March 2023, the local weather in the harbour of Bremerhaven underwent another abrupt meteorological change, with several abrupt shifts in air temperature, wind speed, and precipitation (Fig. 3e, g). During the operation of the ASV, the wind speed sharply increased to 6.53, 10.49 and 9.21 m s^{-1} at 07:58, 08:29 and 10:41 UTC, respectively (Fig. 3e). Afterwards, notable decreases in air temperature of –0.5, –1.4 and –2.4 °C were observed at 08:14, 08:56 and 10:53 UTC, respectively (Fig. 3e, Table 1). The wind direction shifted multiple times from North–West to South–West (Fig. S4). During the most pronounced decrease in air temperature, the wind speed and wind direction stabilised, blowing steadily from the West–North–West to North–West. Coincidentally, with each abrupt meteorological change, the precipitation rate increased rapidly (Fig. 3g). The highest precipitation rate occurred with the largest decrease in air temperature, with a maximum precipitation rate of 1.24 mm h^{-1}. Figure S5 shows that the accumulated evaporation was consistently higher than the accumulated precipitation, indicating a positive evaporation–precipitation flux.

The surface temperature showed three abrupt decreases concurrently with the observed reduction in air temperature and net heat flux and an increase in wind speed (Fig. 3a, e, and f). The temperature at the 100 cm depth was warmer over the entire observation than the skin layer temperatures, resulting in a cool skin layer of 4.85 ± 0.14 °C. A higher temperature occurred at the 100 cm depth, with a mean temperature of 5.22 ± 0.14 °C, resulting in a general skin anomaly temperature of –0.36 ± 0.07 °C. Following an increase in wind speed (Fig. 3e), the skin temperature anomalies reached their maximum at 08:08 UTC with a value of –0.67 °C, at 08:35 UTC with a value of –0.63 °C, and at 10:56 UTC with a value of –0.54 °C.

A more saline skin layer was observed throughout most of the operational period compared with the 100 cm depth. The mean salinity during the observation was 09.12 ± 0.24 g kg^{-1} in the skin layer and 9.07 ± 0.07 g kg^{-1} at the 100 cm depth. A decrease in skin salinity was observed only at higher wind speeds, with values reaching those observed at the 100 cm depth, resulting in salinity anomalies close to zero (Fig. 3e). During the three abrupt meteorological changes with increasing wind speed (Fig. 3e), salinity anomalies were removed, and the skin layer and the 100 cm depth showed similar salinity. The density of the skin layer was consistently higher than that at the 100 cm depth, with a mean density of 1,007.21 ± 0.26 kg m^{-3} in the skin layer and 1007.16 ± 0.19 kg m^{-3} at the 100 cm depth. In general, the observed pattern aligned with the trend in salinity fluctuations.

Latent and sensible heat fluxes were consistent, with notable decreases occurring concurrently with periods of elevated wind speeds (Fig. 3f). The strongest reduction of the net heat flux of –252 W m^{-2} was observed approximately 7 min later than the largest air temperature decreases and wind speed increases (10:41 UTC and 10:53 UTC). At that time, the net heat flux became negative (–79 W m^{-2}) and the shortwave heat flux showed the largest decrease of –208 W m^{-2}. The latent and sensible heat fluxes decreased notably from –13.36 and –4.93 W m^{-2} to –72 and –50 W m^{-2}, respectively.

https://doi.org/10.5194/egusphere-2025-1307
Preprint. Discussion started: 27 March 2025

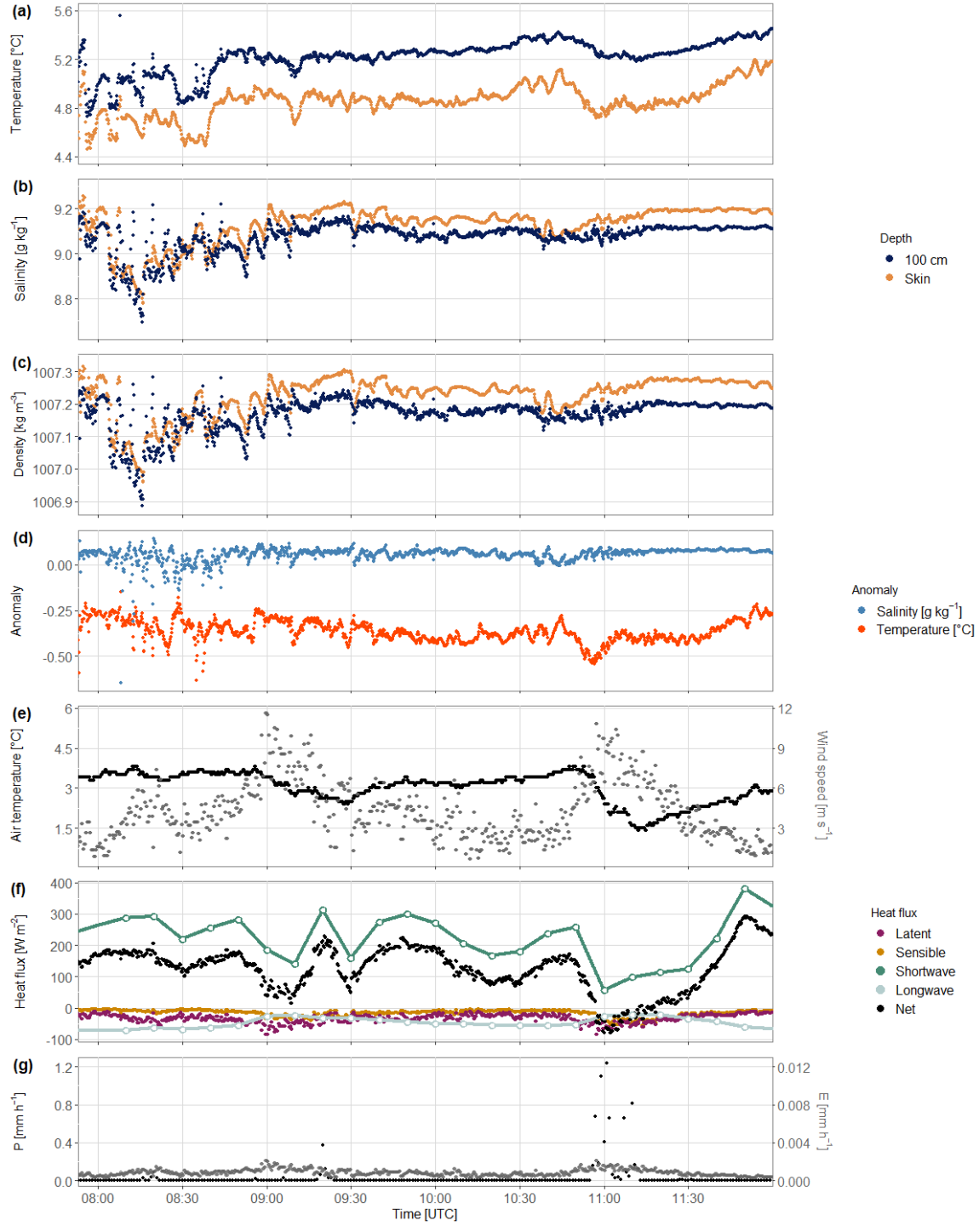

Figure 3: Time series of (a) sea surface temperature, (b) sea surface salinity, (c) sea surface density, (d) temperature and salinity anomaly, (e) air temperature and wind speed, (f) heat flux components, (g) precipitation (P) and evaporation (E) rates on 15 March 2023.

https://doi.org/10.5194/egusphere-2025-1307
Preprint. Discussion started: 27 March 2025

3.2.2 Current velocities on the surface

From 08:00 to 11:45 UTC on 15 March 2023, the zonal velocity component indicated alternating flow patterns, with eastward and westward flows occurring intermittently throughout the observation period (Fig. 4a). Notable variability in the flow was observed over depth, with shear layers developing particularly at depths of approximately 3–4 m. The meridional velocity component exhibited a dynamic vertical structure (Fig. 4b). Early in the observation period, a northward flow dominated at greater depths. By contrast, a southward flow was more pronounced near the surface. As the period progressed, shifts in flow direction occurred, with the southward flow extending further into the water column and the northward flow retreating to lower depths. The backscatter intensity indicated clear temporal and depth-related variabilities (Fig. 4c). Enhanced backscatter values were evident near the surface after 09:30 UTC, suggesting that increased particle concentrations or turbulence were likely increased by precipitation and wind-induced mixing. Below the 2.5 m depth, the backscatter intensity remained relatively stable.

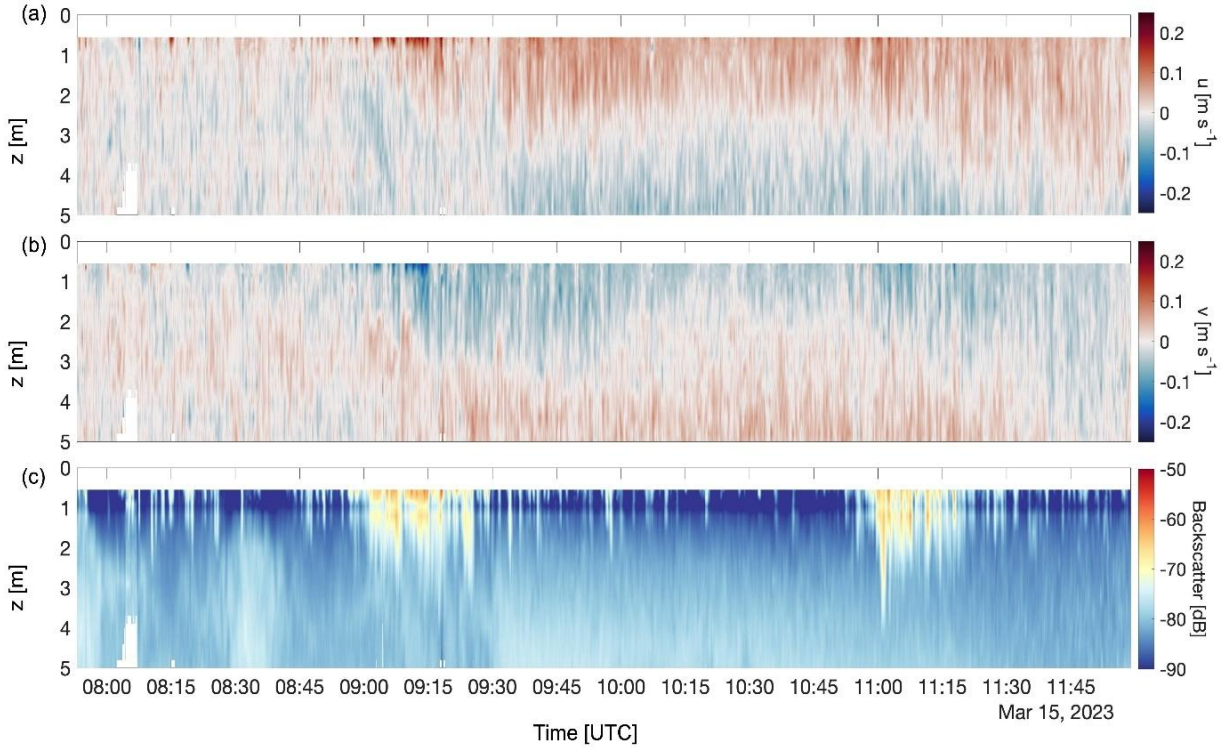

Figure 4: Current velocity data measured with an ADCP mounted at the centre of HALOBATES on 15 March 2023. (a) Zonal current velocity, (b) meridional current velocity and (c) backscatter signals are shown in three panels, and the colour scale shows the velocity magnitude for each current velocity component.

https://doi.org/10.5194/egusphere-2025-1307
Preprint. Discussion started: 27 March 2025

3.3 North Sea event on 10 October 2022

3.3.1 Thermohaline features during abrupt meteorological changes

Figure 5 shows that abrupt meteorological changes altered the thermohaline structures on the sea surface in the North Sea on 10 October 2022. The meteorological variables changed rapidly at approximately 14:00 UTC (Fig. 5e–g). The air temperature decreased from 14.4 to 12.7 °C within 30 min (Fig. 5e). Before the abrupt meteorological change, the average air temperature was 14.51 ± 0.12 °C. After the abrupt change, the air temperature was 13.14 ± 0.05 °C. within 10 min (Fig. 5e). Between 14:20 and 14:30 UTC, the minimum wind speed was 5.8 m s^{-1}, and the maximum wind speed was 15.0 m s^{-1}, indicating a wind speed increase of 9.2 m s^{-1} within 10 min. Before the abrupt meteorological change, the average wind speed was 8.79 ± 0.49 m s^{-1} and 10.30 ± 1.04 m s^{-1} thereafter. At the same time, the wind speed increased, and the wind direction changed slightly from East to East–South–East (Fig. S6). The precipitation rate reached a maximum of 10.57 mm h^{-1} at 14:15 UTC. After the abrupt meteorological change, the accumulated precipitation greatly exceeded the accumulated evaporation (Fig. S7).

Initially, the surface temperature in the skin layer and the 100 cm depth decreased slightly until the weather changed abruptly at 14:00, and the temperature then continued to decrease slowly (Fig. 5e–g). The temperature in the skin layer and the 100 cm depth decreased further, with the largest decrease of –0.15 °C in the skin layer at 14:09 UTC (Fig. 5a). The skin temperature anomaly was, on average, 0.02 ± 0.01 °C before and –0.05 ± 0.02 °C after the abrupt meteorological change (Fig. 5d). Thus, a cool skin layer evolved, with a maximum skin anomaly of –0.12 °C at 14:47 UTC. The salinity decreased slightly by 0.05 g kg^{-1} during the entire measurement time at all depths (Fig. 5b). At 14:11 UTC, the surface temperature dropped abruptly, and the salinity decreased rapidly; simultaneously, the highest precipitation rates occurred. This decrease was most pronounced in the skin layer, with a maximum salinity anomaly of –0.16 g kg^{-1} at 14:16 UTC (Fig. 5d). The density of the skin layer was lower than that at the 100 cm depth before the abrupt meteorological changes (Fig. 5c). During the abrupt change, skin density decreased quickly by 0.12 kg m^{-3} within approximately 8 min and was higher after the abrupt decrease in air temperature. The average density of the skin layer was 1024.09 ± 0.00 kg m^{-3} before the meteorological change and 1024.11 ± 0.01 kg m^{-3} afterwards. The density at the 100 cm depth remained constant, with a mean of 1024.10 ± 0.00 kg m^{-3} during the ASV observation.

The latent, sensible and net heat fluxes decreased by 48 W m^{-2}, 32 W m^{-2} and 100 W m^{-2}, respectively. The shortwave heat flux was low over the entire time series and increased at the end (between 15:00 and 15:20 UTC) to a mean value of 104 W m^{-2} (Fig. 5f). At the end of the deployment, the net heat flux increased from –153 W m^{-2} to –49 W m^{-2}. The longwave heat flux was stable with slightly negative values, with a mean of –18 ± 5 W m^{-2}.

https://doi.org/10.5194/egusphere-2025-1307
Preprint. Discussion started: 27 March 2025

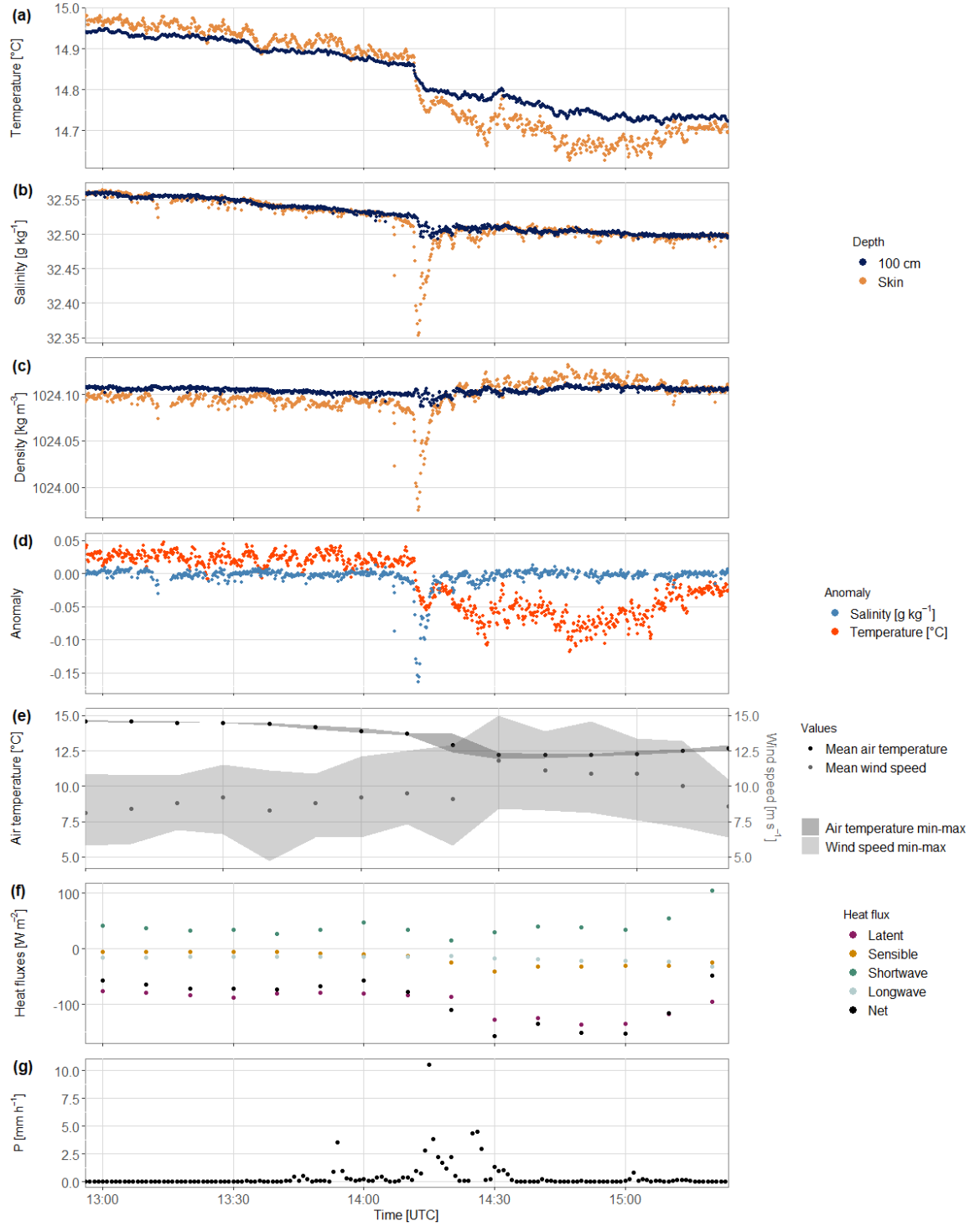

Figure 5: Time series of (a) sea surface temperature, (b) sea surface salinity, (c) sea surface density, (d) temperature and salinity anomaly, (e) mean air temperature and wind speed with minimum and maximum values, (f) heat flux components and (g) precipitation (P) rates on 10 October 2022.

https://doi.org/10.5194/egusphere-2025-1307
Preprint. Discussion started: 27 March 2025

3.3.2 Current velocities on the surface

Figure 6 shows the time-depth plots derived from the ADCP data collected on 10 October 2022, highlighting the eastward (u) and northward (v) velocity components and the backscatter intensity over the observation period from 13:00 to 15:15 UTC from the surface to the 5 m depth. The entire profile of the maximum depth is shown in Figure S8. The eastward velocity component (u) revealed a predominantly westward flow throughout the water column, represented by the negative values in blue. This westward flow intensified with depth, reaching magnitudes of approximately –0.4 m s^{-1}. The northward velocity component (v) exhibited alternating flow directions over time and depth. Northward flows, depicted in red, and southward flows, shown in blue, occurred intermittently, with significant variability in the upper layers of the water column.

Conversely, in the deeper layers between 13:15 and 14:15 UTC, the currents predominantly shifted in a southward direction, indicating the presence of a significant shearing layer around a depth of 2 m. After 14:15 UTC, the currents shifted southward again, with notable shear observed in the first metre in the southward direction. The backscatter intensity plot reflects notable spatial and temporal differences in suspended particle concentrations (Fig. 6c). The backscatter intensity was elevated near the surface, denoted by the yellow and red regions (Fig. 6c), indicating higher particle concentrations or dynamic mixing processes, possibly driven by surface wind or wave activity. Below a depth of 2 m, the backscatter intensity was lower and more consistent, with minimal fluctuations over time. Overall, the plots provide a detailed depiction of the temporal and vertical variations in flow dynamics and particle distribution, offering valuable insights into the hydrodynamic processes occurring in the study area during the observed period.

https://doi.org/10.5194/egusphere-2025-1307
Preprint. Discussion started: 27 March 2025

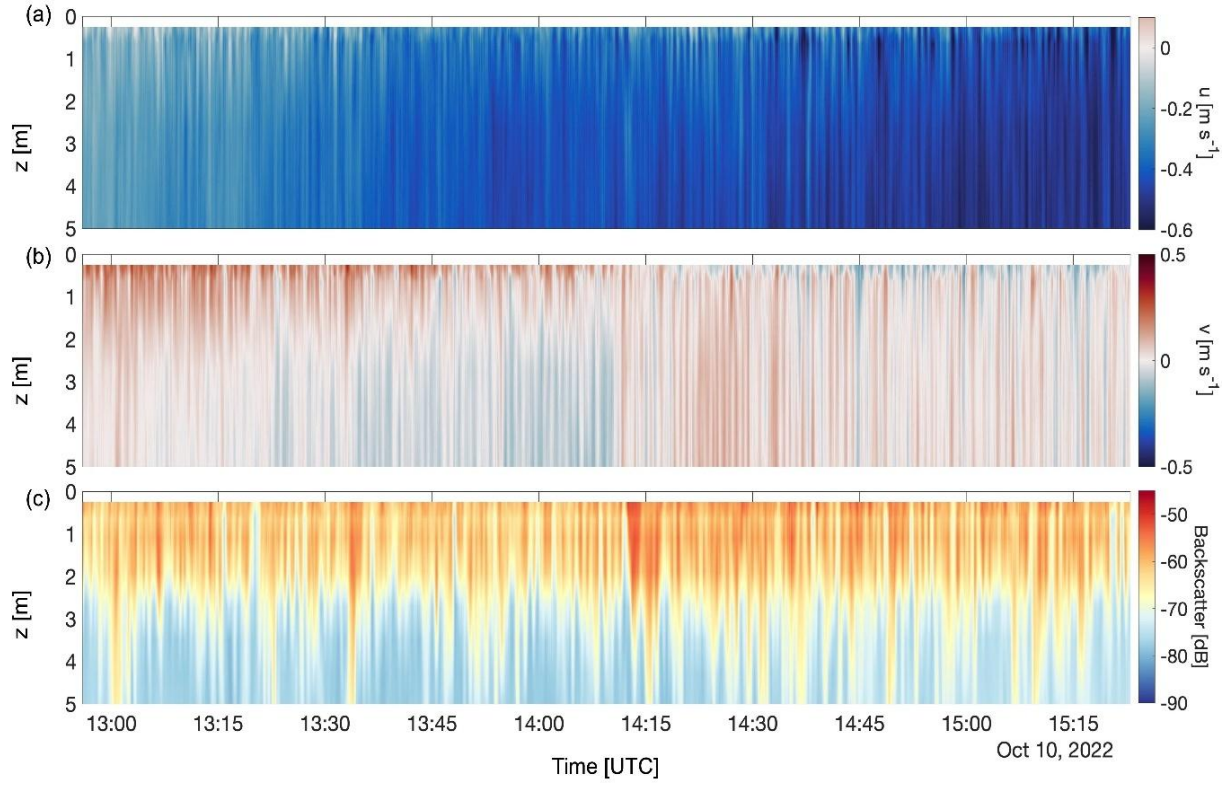

Figure 6: Current velocity data measured with an ADCP mounted at the centre of HALOBATES on 10 October 2022. (a) Zonal current velocity, (b) meridional current velocity and (c) backscatter signals are shown in three panels, and the colour scale shows the velocity magnitude for each current velocity component. For a better comparison with the harbour events, only the upper 5 m are shown.

3.4 Correlation analysis of temperature and salinity anomalies with meteorological parameters

The correlation heat map after the Pearson correlation analysis from the harbour events on 14 and 15 March 2023 and from the North Sea event on 10 October 2022 (Fig. 7a–c) shows that all events had a negative correlation between temperature anomalies and wind speed and a positive correlation between temperature anomalies and air temperature and net heat flux. Regarding these results, the correlation of the events on 14 March 2023 and 10 October 2022 was stronger than that on 15 March 2023. The temperature anomaly showed only a significant negative but weak correlation with precipitation on 15 March 2023 (Fig. 7b).

The correlation analysis of the harbour event on 14 March 2023 (Fig. 7a) revealed a weak correlation between salinity anomalies and meteorological variables. Wind speed demonstrated a significant, although weak, positive correlation with the salinity anomalies, while the net heat flux exhibited a weak and negative correlation with the salinity anomalies of the first harbour event. The North Sea measurements revealed significant positive correlations between salinity anomalies, air temperature, and net heat flux. Conversely, a significant negative correlation was observed between salinity anomalies, wind speed, and precipitation intensity. The correlation analysis also showed a weak but significant positive correlation between

https://doi.org/10.5194/egusphere-2025-1307
Preprint. Discussion started: 27 March 2025

salinity anomalies and backscatter signals during the harbour events. The North Sea event was the only event that showed a significant negative correlation between salinity anomalies and precipitation (Fig. 7c).

Furthermore, the net heat flux showed a strong negative correlation with wind speed during all events. The correlation between net heat flux and air temperature was significant in all cases. The results showed a strong positive correlation during the first harbour event (14 March 2023) and a weak correlation during the second harbour event and the North Sea event. The correlation between air temperature and wind speed was significant during all events, with a strong correlation during the first harbour and North Sea events. The correlation analysis revealed positive but weak correlations between wind speed and backscatter signals.

https://doi.org/10.5194/egusphere-2025-1307
Preprint. Discussion started: 27 March 2025

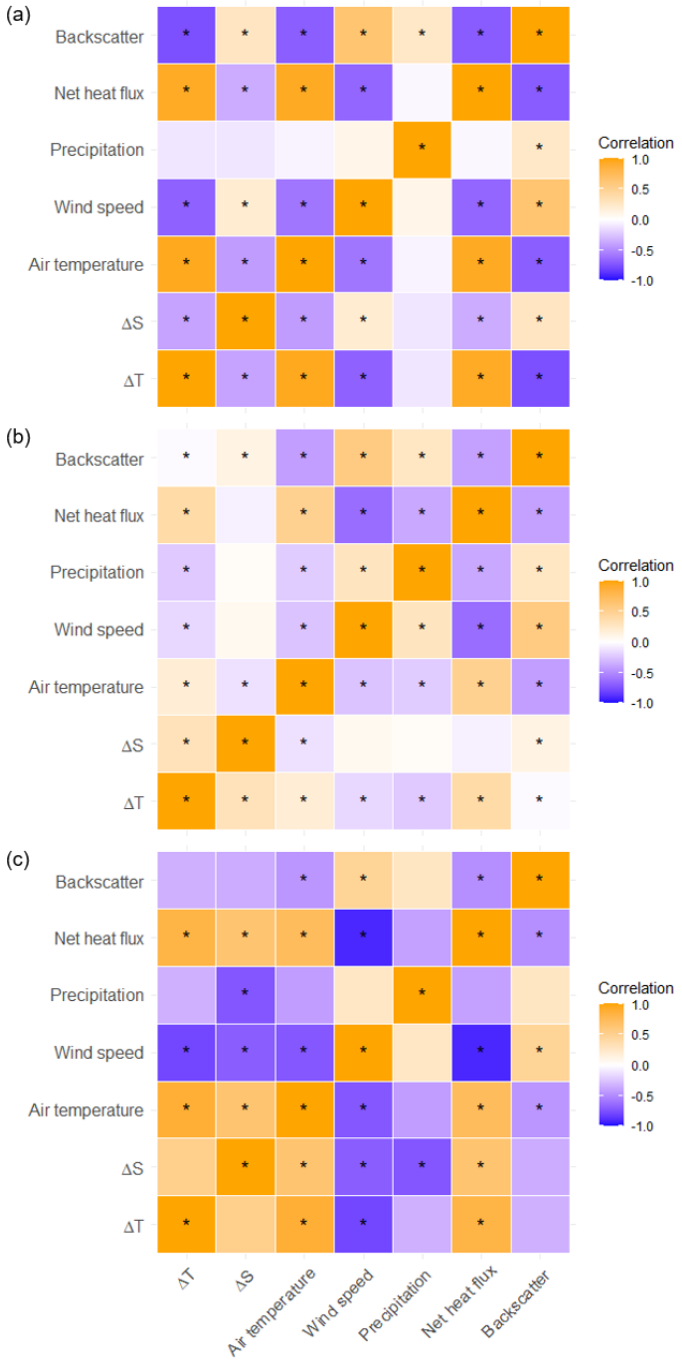

Figure 7: Correlation heat map after the Pearson correlation analysis from (a) the harbour event on 14 March 2023, (b) the harbour event on 15 March 2023 and (c) the North Sea event on 10 October 2022. Each cell represents the correlation strength and direction between two variables, with different colours indicating the degree of correlation: warm colours (orange) for positive and cold colours (blue) for negative correlations. The colour intensity reflects the magnitude of the correlation, ranging from –1 (strong negative correlation) to +1 (strong positive correlation). Significant correlations ($p < 0.05$) are annotated with an asterisk.

https://doi.org/10.5194/egusphere-2025-1307
Preprint. Discussion started: 27 March 2025

4 Discussion

The findings of this study offer significant insights into the effects of abrupt meteorological changes on temperature and salinity anomalies. All three events of an abrupt meteorological change showed abrupt shifts in air temperature, wind speed, heat flux, and precipitation. The harbour events (14–15 March 2023) had a more pronounced decrease in air temperature than the North Sea event (10 October 2022). Abrupt changes in the net heat flux, mainly driven by changes in latent and sensible heat fluxes, coincided with changes in air temperature and wind speed. These fluctuations in the heat exchange between the sea surface and the atmosphere play a critical role in local energy budgets and can influence larger-scale climate patterns (Yu, 2007; Chou et al., 2000). An increase in wind speed was observed in all events, with the North Sea event showing higher overall wind speeds. Precipitation patterns varied across the events, affecting salinity only with the highest observed precipitation intensities. The duration and intensity of meteorological changes differed between the harbour and North Sea events, highlighting the importance of local conditions. While the responses of the skin layer to the investigated abrupt meteorological changes were characterised by cooling, the salinity responses, particularly in the harbour events, indicated a complex interplay of factors, including wind speed and freshwater inputs. Temperature and salinity anomalies are further discussed in Sections 4.1. and 4.2. The density during the harbour events in the skin layer was always slightly higher than that at the 100 cm depth, which indicates that the skin layer has special properties compared with the NSL, forcing these differences and avoiding mixing with the underlying water. The relationship between the density differences and the influence of wind and evaporation revealed complex and dynamic processes, which are further examined in Section 4.3.

4.1 Effects on temperature anomalies

Across all three events, the sudden decreases in air temperature resulted in corresponding reductions in the sea surface temperature, with the skin layer exhibiting a more pronounced cooling than the 100 cm depth (Table 1). Cool skin anomalies developed or intensified after weather changes in all events, with varying magnitudes and durations. Except for the first abrupt meteorological change on 15 March 2023, which was the less pronounced event compared with the other events (Table 1), the decline in temperature within the skin layer exhibited a considerable decrease compared with the 100 cm depth in all events. The average temperature change at the 100 cm depth corresponded to 48.4% of the temperature change observed in the skin layer, indicating a disproportionately greater cooling effect in the skin layer than in the subsurface water. This shows that the temperature change in the skin layer caused by abrupt meteorological changes is underestimated by almost 50% when measured at a depth of 100 cm. This underscores the importance of measuring these processes directly at the air–sea boundary layer and developing models to predict the effects of such events accurately.

During the first harbour event (14 March 2023), a positive net heat flux was observed before the meteorological change, mainly governed by incoming solar radiation. Nevertheless, the skin temperature anomaly was slightly negative, most likely caused by precipitation. In many cases, the precipitation temperature is cooler than the surface temperature, which can have a cooling effect (Gosnell et al., 1995). Studies have shown that the skin layer responds to precipitation first and is most pronounced

https://doi.org/10.5194/egusphere-2025-1307
Preprint. Discussion started: 27 March 2025

compared with the NSL (Wurl et al., 2019; Gassen et al., 2024a; Gassen et al., 2024b). The precipitation intensity showed an insignificant negative correlation with the temperature anomalies (Fig. 7a). The low precipitation rates could have caused the insignificance of the relationship during this event. Nevertheless, before the abrupt meteorological change, the light precipitation likely caused a slightly cooler skin layer by –0.09 °C than the 100 cm depth. After the abrupt meteorological change, sensible, latent, and longwave heat fluxes became negative; consequently, the mean net heat flux decreased to –3 ± 17 W m^{-2}, further cooling the skin layer. Simultaneously, the temperature anomaly abruptly decreased by –0.32 °C as the heat fluxes and the air temperature decreased with a concomitant increase in wind speed. The correlation analysis confirmed this, showing a significant positive correlation between temperature anomaly, air temperature, and net heat flux (Fig. 7a). Wind speed showed a strong and significant negative correlation.

During the second harbour event (15 March 2023), a cooler skin layer was present throughout the measurement period. The meteorological features changed abruptly three times during the observation, and every time, a decrease in air temperature was observed with a simultaneous increase in wind speed (Fig. 3). At the same time, the net heat flux decreased by –81, –182 and –252 W m^{-2}, leading to further reductions in skin temperature by –0.32, –0.29 and –0.40 °C, respectively. Compared with the first harbour event on 14 March 2023, the positive correlation of the temperature anomalies with air temperature and net heat flux was less pronounced but remained significant (Fig. 7b). The correlation between the temperature anomalies and the wind speed was negative and significant but also less pronounced compared with the first event. The frequency and intensity between the abrupt meteorological changes of the events most likely caused these less pronounced linear relationships. For example, on 15 March 2023, several shorter abrupt meteorological changes occurred. Compared with the event on 14 March 2023, in which one very pronounced abrupt meteorological change occurred, the correlation analysis revealed a weaker correlation.

During the North Sea event (10 October 2022), the skin temperature was, on average, slightly higher than that at the 100 cm depth, resulting in a positive temperature anomaly before the abrupt meteorological change. With a decreasing air temperature and increasing wind speed, the temperature anomaly decreased, and a cooler skin developed. This is confirmed by the strong positive correlation between temperature anomalies and net heat flux (Fig. 7c). Wind speed showed a significant negative correlation with temperature anomalies. The North Sea event demonstrated larger magnitudes in the correlation analysis than did the harbour events, possibly due to the greater wind speeds encountered in the open sea environment. Elevated wind speeds were observed in all events, leading to enhanced mixing in the upper water column. This increased turbulence is crucial in the vertical transport of heat, mass, and momentum within the ocean (Qiao et al., 2016). Donlon et al. (1999) observed the development of cool skin with a mean temperature anomaly of 0.14 °C and wind speeds > 6 m s^{-1}. Open sea events are more likely to exhibit higher overall wind speeds than harbour events because of the absence of land-based obstacles and the larger fetch available for wind development.

In addition, the seasonal difference between the harbour events (March) and the North Sea event (October) could have contributed to the disparity in the magnitude of the correlation analysis. Seasonal variations in air and water temperatures and atmospheric conditions can significantly influence the air–sea exchange processes (Wallace et al., 1989). March, which is typically associated with the transition from winter to spring, may have different temperature gradients and atmospheric

https://doi.org/10.5194/egusphere-2025-1307
Preprint. Discussion started: 27 March 2025

stabilities than October, which often marks the transition from autumn to winter (Wu and Chen, 2020). Combined with the distinct characteristics of sea and harbour environments, these seasonal factors could explain the observed differences in the correlation analysis. Although our study is based on a limited number of observations, these cases provide valuable insights into the effects of abrupt meteorological changes on the skin layer.

The ADCP data revealed complex current patterns and vertical shear in response to changing wind conditions. These observations emphasize the intricate relationship between atmospheric forcing and oceanic circulation patterns. Vertical shear in current velocities was observed, which has implications for turbulent mixing and energy dissipation. Increased backscatter intensity near the surface during precipitation suggests enhanced mixing or particle concentration, potentially affecting air–sea heat fluxes. The response of currents to meteorological changes varied among events, providing insights into the local dynamics of momentum transfer.

The results showed that cool skin conditions emerged following abrupt meteorological changes, with persistent negative skin temperature anomalies. In all cases, the wind speed increased with changing weather conditions, causing the net heat flux to decrease. The temperature changes in the skin layer increased disproportionally to the temperature at the 100 cm depth, intensifying near-surface stratification. This emphasises the importance of accounting for skin layer dynamics in air–sea interaction studies and climate models. Furthermore, the correlation analysis (Fig. 7) showed some differences between the events. The limited water volume and reduced circulation in the harbour could have contributed to more pronounced temperature fluctuations. Tidal dynamics influence the North Sea, but during operational time, there was no change in the tidal direction, and it was assumed to be stable.

All events showed a negative correlation between temperature anomalies and wind speed and a positive correlation between temperature anomalies and air temperature and net heat flux. The interaction between heat fluxes and surface temperature is a complex and dynamic process that plays a crucial role in understanding climate systems and energy balance. As Webster et al. (1996) highlighted, even a change of 1 °C in skin temperature could significantly alter the net surface heat flux of 27 W m^{-2}. This relationship is bidirectional, with the heat fluxes influencing the surface temperature and vice versa, creating a feedback loop. Our results show that although abrupt meteorological changes are relatively rare on a global scale, they can dramatically intensify heat flux variations or even cause a complete reversal, thus emphasising the importance of capturing these events to improve climate models and energy balance estimates.

However, the rapid response of skin temperature in all events highlights the sensitivity of the ocean's uppermost layer to atmospheric changes. Sensible heat flux depends highly on air temperature (Fairall et al., 1996b). Higher gradients between air temperature and surface temperature cause a higher sensible heat flux. Fairall et al. (1996b) showed that a warmer surface temperature than an air temperature causes a negative sensible heat flux in the atmosphere. Many studies have investigated the changes in sea surface temperature across various timescales, from daily to annual, primarily focusing on diurnal to seasonal variations (Folland and Parker, 1990; Cayan, 1992; Sura et al., 2006). Gill and Niller (1973) concluded that temperature anomalies are predominantly driven by heat flux through the sea surface.

https://doi.org/10.5194/egusphere-2025-1307
Preprint. Discussion started: 27 March 2025

This study is the first to examine small-scale changes in the skin layer caused by abrupt meteorological shifts. The findings underscore the critical importance of including the skin layer in future research, as changes induced by meteorological shifts could be underestimated when measuring depths of several metres, potentially leading to inaccurate analyses of surface temperatures and the effects of heat and gas fluxes (Börner et al., 2022). The significance of this research is further amplified by the potential increase in extreme weather events due to climate change (Allen and Ingram, 2002; Ummenhofer and Meehl, 2017). As Francis and Skific (2015) suggested, disproportionate Arctic warming could lead to more meridional characteristics in Northern Hemisphere circulation, potentially increasing the frequency of such events. Consequently, future studies should prioritize high-resolution measurements of the skin layer to accurately capture these abrupt changes. By including these fine-scale processes, a mechanistic understanding of heat fluxes in the skin layer can be enhanced.

4.2. Effects on salinity anomalies

The harbour events exhibited changes in salinity in the skin layer and at the 100 cm depth after abrupt weather changes, with the skin layer consistently displaying the highest change in salinity, except for two events (Table 1). The salinity in the harbour events sometimes increased and decreased with abrupt meteorological changes. By contrast, the North Sea event demonstrated a slight decrease in salinity, with the most pronounced reduction occurring in the skin layer. On 14 March 2022, the salinity increased in the skin layer and at the 100 cm depth, possibly because of enhanced vertical mixing or the advection of saltier water. On 15 March 2022, the salinity differences between the skin layer and the 100 cm depth were removed during periods of high wind speed, indicating strong mixing processes consistent with the results of the flow velocities and backscatter signals. The correlation analysis confirmed a weak but significant positive correlation between salinity anomalies and backscatter signals. Although wind-induced mixing was stronger, the North Sea event demonstrated a slight decrease in salinity with abrupt meteorological changes, with the most pronounced change in the skin layer. This reduction was likely caused by a strong precipitation intensity and high accumulated precipitation, which was forced to freshen the sea surface (Gassen et al., 2024b). This was the only event during which salinity anomalies showed a significant negative correlation with precipitation (Fig. 7c). Overall, the salinity in the harbour was 8–9 g kg^{-1}, which is much lower than that of the North Sea because the harbour basin is influenced by freshwater input.

The correlation analysis of the first harbour event on 14 March 2023 (Fig. 7a) revealed a weak correlation between salinity anomalies and meteorological variables. The wind speed showed a significant, although weak, positive correlation with salinity anomalies. The net heat flux correlated weakly and negatively with the salinity anomalies of the first harbour event. The North Sea measurements showed significant positive correlations between salinity anomalies and both air temperature and net heat flux, indicating that warmer conditions and increased heat transfer at the air–sea interface could contribute to higher salinity in open waters (Fig. 7c). A significant negative correlation was observed between salinity anomalies and both wind speed and precipitation intensity.

https://doi.org/10.5194/egusphere-2025-1307
Preprint. Discussion started: 27 March 2025

These findings highlight the complex interplay between the environmental factors influencing salinity dynamics in marine environments. This shows that in the observation of abrupt meteorological shifts in salinity, the harbour environment is less comparable with the North Sea conditions than the surface temperature changes because the salinity is very different. Complex shear currents caused by the enclosed harbour basin could cover the effects of net heat flux on salinity anomalies.

4.3. Characteristics of the skin layer and their relation to density variations

The distinct thermohaline properties of the skin layer, which are known for their unique biogeochemical properties that differ from those of the underlying seawater (Wurl et al., 2011), have become particularly visible in these observations. The skin layer is a critical boundary between the ocean and the atmosphere, directly influenced by continuous exchange processes, such as heat, gas and freshwater fluxes (Schlüssel et al., 1997). With increasing wind speed, evaporation rates also increase, leading to the removal of latent heat and freshwater and, consequently, the development of a cooler skin layer (Murray et al., 2000). This cooling effect was notably observed during the harbour events and after the abrupt meteorological change in the North Sea event. During the harbour events, a cool and more saline skin layer was observed, which was more pronounced following abrupt meteorological changes. Cooler skin developed after abrupt meteorological changes during the North Sea event. Unlike in the harbour events, saltier skin was not observed because of the input of freshwater through precipitation.

In our observations, the density of the skin layer was mainly consistently higher than that at the 100 cm depth, with mean density differences of 0.05 kg m^{-3} for the harbour events and 0.02 kg m^{-3} for the North Sea event, underscoring its distinct characteristics. Wurl et al. (2019) also observed a denser skin layer compared with the 100 cm depth in the tropical Pacific region. They found a density anomaly (skin – 100 cm) threshold of 13 kg m^{-3} in which the interfacial tension could hold the denser skin layer afloat the NSL. This was confirmed by Gassen et al. (2023), who observed density anomalies of up to 10 kg m^{-3}. Laboratory experiments and theoretical modelling further support these observations, demonstrating that denser fluids can float atop water surfaces due to interfacial tension (Singh and Joseph, 2005; Phan et al., 2012; Phan, 2014), reinforcing the unique interplay between the skin layer's physical properties and its response to environmental dynamics. Our observed density anomalies are much lower than those of Wurl et al. (2019) and Gassen et al. (2023), suggesting that the surface tension is strong enough to maintain the denser skin layer over the NSL in our case, despite the increasing wind speeds and heat fluxes, which further increased the density differences to some extent.

5. Conclusions

The findings of this investigation offer significant insights into the effects of abrupt meteorological changes on temperature and salinity anomalies in both harbour and sea environments at mid-latitudes. This study reveals the intricate relationships between atmospheric conditions and sea surface responses, providing valuable information for understanding air–sea

https://doi.org/10.5194/egusphere-2025-1307
Preprint. Discussion started: 27 March 2025

interactions and their implications for local and regional climate dynamics. These observations highlight the complex and rapid response of the ocean skin layer to abrupt meteorological changes and show its distinct thermohaline properties, demonstrating its cooler and denser characteristics compared with underlying seawater, particularly in response to meteorological changes and varying environmental conditions. The temperature sensitivity of the skin layer to atmospheric forcing was almost 50% higher than that of the 100 cm depth. This emphasises the importance of the skin layer in air–sea interactions.

Although we observed differences between the harbour and open sea environments, analysing the temperature anomalies enhanced the mechanistic understanding of small-scale processes at the air–sea interface. The harbour environment can be regarded as a large-scale mesocosm, providing a controlled yet dynamic setting for studying complex physical processes under natural conditions. This understanding is crucial for improving climate models and weather forecasting systems. In all cases, a significant and strong correlation was observed between the temperature anomalies and both air temperature and wind speed at the air–sea boundary layer. A similar relationship was also identified in the heat fluxes at the boundary layer, underscoring the necessity of considering the combined influences of all factors to comprehensively understand the effects of meteorological events on surface conditions, thereby highlighting the dynamics of the skin layer. However, the limited number of observed events and the differences in environmental conditions present challenges for directly comparing and generalising the findings. Nevertheless, our findings underscore the need for high-resolution monitoring systems that capture abrupt changes in atmospheric and oceanic parameters, including the ocean's skin layer. This study emphasises the importance of further small-scale investigations of the skin layer during abrupt meteorological changes in other regions and of expanding the data in the mid-latitudes for a more robust comparison. Future studies could benefit from longer-term observations and more diverse geographical locations to better understand the variability in skin layer responses to abrupt meteorological changes.

Data availability

All the data generated or analysed during this study is available in this published article and on PANGAEA (Gassen et al., 2024c; Gassen et al., 2025).

Author contribution

LG took the lead in writing the manuscript, analysing data, and designing the figures. LG, OW, SMA and JM conducted field observations and data recording. JM contributed to the writing of the manuscript, data processing, and designing figures. SMA and LJ processed the data and contributed to the analysis of the results. OW supervised the project. All authors discussed the results and commented on the manuscript.

https://doi.org/10.5194/egusphere-2025-1307
Preprint. Discussion started: 27 March 2025

Competing interests

The authors declare that they have no conflict of interest.

Acknowledgements

We would like to thank the captain, the crew and the scientific team on board RV *Heincke* for their support, R. Henkel for carrying out the salinometer measurements, and the Alfred Wegner Institute for providing the salinometer.

Financial support

The work on the RV *Heincke* was funded by the Ministry of Science and Culture of Lower Saxony Ministry of Science and Culture as part of the project The North Sea from Space: Using explainable artificial intelligence to improve Satellite observations of climate change (NorthSat-X) project, Project number VWZN3680. The analysis and the publications writing were carried out as part of Freshwater Fluxes Over the Ocean (FreshOcean) - project number 510639210.

References

Allen, M. R. and Ingram, W. J.: Constraints on future changes in climate and the hydrologic cycle, 10.1038/nature01092, 2002.

Börner, R., Haerter, J. O., and Fiévet, R.: DiuSST: A conceptual model of diurnal warm layers for idealized atmospheric simulations with interactive SST, 10.5194/egusphere-2024-1876, 2022.

Cayan, D. R.: Latent and sensible heat flux anomalies over the northern oceans: Driving the sea surface temperature, 10.1175/1520-0485(1992)022<0859:lashfa>2.0.co;2, 1992.

Chou, S.-H., Zhao, W., and Chou, M.-D.: Surface heat budgets and sea surface temperature in the Pacific warm pool during TOGA COARE, 10.1175/1520-0442(2000)013<0634:shbass>2.0.co;2, 2000.

Donlon, C. J., Nightingale, T. J., Sheasby, T., Turner, J., Robinson, I. S., and Emergy, W. J.: Implications of the oceanic thermal skin temperature deviation at high wind speed, 10.1029/1999gl900547, 1999.

Durack, P. J.: Ocean salinity and the global water cycle, 10.5670/oceanog.2015.03, 2015.

Fairall, C. W., Bradley, E. F., Hare, J. E., Grachev, A. A., and Edson, J. B.: Bulk parameterization of air--sea fluxes: Updates and verification for the COARE algorithm, 10.1175/1520-0442(2003)016<0571:bpoasf>2.0.co;2, 2003.

Fairall, C. W., Bradley, E. F., Rogers, D. P., Edson, J. B., and Young, G. S.: Bulk parameterization of air-sea fluxes for tropical ocean-global atmosphere coupled-ocean atmosphere response experiment, 10.1029/95jc03205, 1996a.

Fairall, C. W., Bradley, E. F., Godfrey, J. S., Wick, G. A., Edson, J. B., and Young, G. S.: Cool-skin and warm-layer effects on sea surface temperature, 10.1029/95jc03190, 1996b.

Folland, C. K. and Parker, D. E.: Observed variations of sea surface temperature, 10.1007/978-94-009-2093-4_2, 1990.

Francis, J. and Skific, N.: Evidence linking rapid Arctic warming to mid-latitude weather patterns, 10.1098/rsta.2014.0170, 2015.

https://doi.org/10.5194/egusphere-2025-1307
Preprint. Discussion started: 27 March 2025

Gassen, L., Esters, L., Ribas-Ribas, M., and Wurl, O.: The impact of rainfall on the sea surface salinity: A mesocosm study, 10.1038/s41598-024-56915-4, 2024a.

Gassen, L., Ayim, S. M., Badewien, T. H., Ribas-Ribas, M., and Wurl, O.: Wind speed effects on rainfall-induced salinity and temperature anomalies at the sea surface microlayer at mid-latitudes, 10.1525/elementa.2024.00004, 2024b.

Gassen, L., Badewien, T. H., Ewald, J., Ribas-Ribas, M., and Wurl, O.: Temperature and Salinity Anomalies in the Sea Surface Microlayer of the South Pacific during Precipitation Events, 10.1029/2023jc019638, 2023.

Gassen, L., Ayim, S. M., Emig, S., Holthusen, L. A., Jaeger, L., Lagemann, M., Lehners, C., Ribas-Ribas, M., and Wurl, O.: High-resolution measurements of essential climate variables in the North Sea from the autonomous surface vehicle HALOBATES during RV Heincke cruise HE609, 10.1594/PANGAEA.968800, 2024c.

Gassen, L., Ayim, S. M., Riaz, B., Edgar, C., Holthusen, L. A., Jaeger, L., Lehners, C., Ribas-Ribas, M., and Wurl, O.: High-Resolution Measurements of Essential Climate Variables in the Harbor of Bremerhaven from the Autonomous Surface Vehicle HALOBATES during RV Heincke Cruise HE614, 10.1594/PANGAEA.974851, 2025.

Gentemann, C. L., Donlon, C. J., Stuart-Menteth, A., and Wentz, F. J.: Diurnal signals in satellite sea surface temperature measurements, 10.1029/2002gl016291, 2003.

Gill, A. E. and Niller, P. P.: The theory of the seasonal variability in the ocean, Deep Sea Research and Oceanographic Abstracts, 141--177, 10.1016/0011-7471(73)90049-1,

Gosnell, R., Fairall, C. W., and Webster, P. J.: The sensible heat of rainfall in the tropical ocean, 10.1029/95jc01833, 1995.

Ho, D. T., Zappa, C. J., McGillis, W. R., Bliven, L. F., Ward, B., Dacey, J. W. H., Schlosser, P., and Hendricks, M. B.: Influence of rain on air-sea gas exchange: Lessons from a model ocean, 10.1029/2003jc001806, 2004.

Jessup, A. T., Zappa, C. J., Loewen, M. R., and Hesany, V.: Infrared remote sensing of breaking waves, 10.1038/385052a0, 1997.

Katsaros, K. B.: The aqueous thermal boundary layer, 10.1007/bf00117914, 1980.

Katsaros, K. B. and Buettner, K. J. K.: Influence of rainfall on temperature and salinity of the ocean surface, 10.1175/1520-0450(1969)008<0015:iorota>2.0.co;2, 1969.

Leibovich, S.: The form and dynamics of Langmuir circulations, 10.1146/annurev.fl.15.010183.002135, 1983.

Liss, P. S. and Duce, R. A.: The sea surface and global change, 10.1017/CBO9780511525025, 1997.

Liss, P. S., Watson, A. J., Bock, E. J., Jähne, B., Asher, W., Frew, N., Hasse, L., Korenowski, G., Merlivat, L., Phillips, L., and others: Report group 1--physical processes in the microlayer and the air-sea exchange of trace gases, 10.1017/cbo9780511525025.002, 1997.

McDougall, T. J. and Barker, P. M.: Getting started with TEOS-10 and the Gibbs Seawater (GSW) oceanographic toolbox, 2011.

Minnett, P. J.: Radiometric measurements of the sea-surface skin temperature: The competing roles of the diurnal thermocline and the cool skin, 10.1080/0143116031000095880, 2003.

Moulin, A. J., Moum, J. N., Shroyer, E. L., and Hoecker-Martínez, M. n.: Freshwater lens fronts propagating as buoyant gravity currents in the equatorial {I}ndian Ocean, 10.1029/2021jc017186, 2021.

Murray, M. J., Allen, M. R., Merchant, C. J., Harris, A. R., and Donlon, C. J.: Direct observations of skin-bulk {SST} variability, 10.1029/1999gl011133, 2000.

Phan, C. M.: Stability of a floating water droplet on an oil surface, 10.1021/la403830k, 2014.

Phan, C. M., Allen, B., Peters, L. B., Le, T. N., and Tade, M. O.: Can water float on oil?, 10.1021/la204820a, 2012.

https://doi.org/10.5194/egusphere-2025-1307
Preprint. Discussion started: 27 March 2025

Price, J. F., Weller, R. A., and Pinkel, R.: Diurnal cycling: Observations and models of the upper ocean response to diurnal heating, cooling, and wind mixing, 10.1029/jc091ic07p08411, 1986.

Qiao, F., Yuan, Y., Deng, J., Dai, D., and Song, Z.: Wave--turbulence interaction-induced vertical mixing and its effects in ocean and climate models, 10.1098/rsta.2015.0201, 2016.

Renfrew, I. A., Moore, G. W. K., Guest, P. S., and Bumke, K.: A comparison of surface layer and surface turbulent flux observations over the Labrador Sea with ECMWF analyses and NCEP reanalyses, 10.1175/1520-0485(2002)032<0383:acosla>2.0.co;2, 2002.

Ribas-Ribas, M., Hamizah Mustaffa, N. I., Rahlff, J., Stolle, C., and Wurl, O.: Sea Surface Scanner {(S3)}: A Catamaran for High-Resolution Measurements of Biogeochemical Properties of the Sea Surface Microlayer, 10.1175/jtech-d-17-0017.1, 2017.

Schluessel, P., Emery, W. J., Grassl, H., and Mammen, T.: On the bulk-skin temperature difference and its impact on satellite remote sensing of sea surface temperature, 10.1029/jc095ic08p13341, 1990.

Schlüssel, P., Soloviev, A. V., and Emery, W. J.: Cool and freshwater skin of the ocean during rainfall, 10.1023/a:1000225700380, 1997.

Shinki, M., Wendeberg, M., Vagle, S., Cullen, J. T., and Hore, D. K.: Characterization of adsorbed microlayer thickness on an oceanic glass plate sampler, 10.4319/lom.2012.10.728, 2012.

Singh, P. and Joseph, D. D.: Fluid dynamics of floating particles, 10.1017/s0022112005003575, 2005.

Soloviev, A. V., Lukas, R., Donelan, M. A., Haus, B. K., and Ginis, I.: The air-sea interface and surface stress under tropical cyclones, 10.1038/srep05306, 2014.

Sura, P., Newman, M., and Alexander, M. A.: Daily to decadal sea surface temperature variability driven by state-dependent stochastic heat fluxes, 10.1175/jpo2948.1, 2006.

ten Doeschate, A., Sutherland, G., Bellenger, H., Landwehr, S., Esters, L., and Ward, B.: Upper ocean response to rain observed from a vertical profiler, 10.1029/2018jc014060, 2019.

Ummenhofer, C. C. and Meehl, G. A.: Extreme weather and climate events with ecological relevance: a review, 10.1098/rstb.2016.0135, 2017.

Wallace, J. M., Mitchell, T. P., and Deser, C.: The influence of sea-surface temperature on surface wind in the eastern equatorial Pacific: Seasonal and interannual variability, 10.1175/1520-0442(1989)002<1492:tiosst>2.0.co;2, 1989.

Watson, A. J., Schuster, U., Shutler, J. D., Holding, T., Ashton, I. G. C., Landschützer, P., Woolf, D. K., and Goddijn-Murphy, L.: Revised estimates of ocean-atmosphere CO2 flux are consistent with ocean carbon inventory, 10.1038/s41467-020-18203-3, 2020.

Webster, P. J., Clayson, C. A., and Curry, J. A.: Clouds, radiation, and the diurnal cycle of sea surface temperature in the tropical western Pacific, 10.1175/1520-0442(1996)009<1712:cratdc>2.0.co;2, 1996.

Williams, E. and Stanfill, S.: The physical origin of the land--ocean contrast in lightning activity, 10.1016/s1631-0705(02)01407-x, 2002.

Wu, R. and Chen, S.: What leads to persisting surface air temperature anomalies from winter to following spring over mid-to high-latitude Eurasia?, 10.1175/jcli-d-19-0819.1, 2020.

Wurl, O., Miller, L., Röttgers, R., and Vagle, S.: The distribution and fate of surface-active substances in the sea-surface microlayer and water column, 10.1016/j.marchem.2009.04.007, 2009.

Wurl, O., Wurl, E., Miller, L., Johnson, K., and Vagle, S.: Formation and global distribution of sea-surface microlayers, 10.5194/bg-8-121-2011, 2011.

https://doi.org/10.5194/egusphere-2025-1307
Preprint. Discussion started: 27 March 2025

Wurl, O., Landing, W. M., Mustaffa, N. I. H., Ribas-Ribas, M., Witte, C. R., and Zappa, C. J.: The ocean's skin layer in the tropics, 10.1029/2018jc014021, 2019.

Wurl, O., Gassen, L., Badewien, T. H., Braun, A., Emig, S., Holthusen, L. A., Lehners, C., Meyerjürgens, J., and Ribas, M. R.: HALOBATES: An Autonomous Surface Vehicle for High-Resolution Mapping of the Sea Surface Microlayer and Near-Surface Layer on Essential Climate Variables, 10.1175/jtech-d-24-0021.1, 2024.

Yu, L.: Global variations in oceanic evaporation (1958--2005): The role of the changing wind speed, 10.1175/2007jcli1714.1, 2007.

Zappa, C. J., Jessup, A. T., and Yeh, H.: Skin layer recovery of free-surface wakes: Relationship to surface renewal and dependence on heat flux and background turbulence, 10.1029/98jc01942, 1998.